DOI: 10.1002/ejic.201001300

Chemoselective Aerobic Diol Oxidation by Palladium(II)–Pyridine Catalysis

Lorenzo Bettucci,[a] Claudio Bianchini,[a] Jonathan Filippi,[a] Alessandro Lavacchi,[a] and Werner Oberhauser*[a]

Keywords: Oxidation / Palladium / N ligands / Chemoselectivity / Diols

Neutral and cationic palladium complexes that bear pyridine ligands [i.e., pyridine (Py), 4-ethylpyridine (4-EtPy) and 2,4,6-trimethylpyridine (2,4,6-Me_3Py)] have been isolated and characterized in solution by ^{1}H and ^{13}C{^{1}H} NMR spectroscopy, cyclic voltammetry (CV) and in the solid state by elemental analysis and single-crystal structure analysis. All palladium compounds have been scrutinized as a precursor to catalyze the aerobic oxidation of diols either in the presence or in the absence of an external base (i.e., K_2CO_3). As a result, the chemoselective production of the corresponding hydroxy ketones has been achieved. The bis-cationic palladium complex of the formula [Pd(4-EtPy)$_4$](OTs)$_2$ (OTs = *p*-toluenesulfonate) [**5b(OTs)$_2$**] emerged as the most promising precursor; it outperformed the neutral precursor that consisted of *trans*-[Pd(OAc)$_2$(4-EtPy)$_2$] (OAc = acetate) and 4-EtPy [**3b/2(4-EtPy)**] (2 mol-equiv.). An operando high-pressure (HPNMR) spectroscopic study with the precursor **5b(OTs)$_2$** combined with the results obtained from catalytic reactions has provided insight into the catalytic mechanism that is operative in **5b(OTs)$_2$**-catalyzed aerobic diol oxidation reactions.

Introduction

Since the discovery of palladium-catalyzed aerobic alcohol oxidation by Schwartz et al.,[1] increasing research has being carried out to develop palladium-based catalysts for the oxidation of alcohols to either ketones or aldehydes, which represents a key transformation in many organic synthesis protocols.[2] The circumvention of traditionally applied organic oxidants, currently used in stoichiometric amounts,[3] or of toxic metals[4] is mandatory for a green chemistry approach to organic synthesis. Oxygen or air have already found wide application as final hydrogen acceptors in palladium-catalyzed alcohol oxidation reactions.[5] Among the various palladium-based homogeneous complexes used as precursors for aerobic alcohol oxidation, Sheldon and co-workers' palladium-neocuproin[5b,5g] and palladium-bathocuproin system[5f] as well as Uemura and co-workers' palladium-pyridine precatalyst[5i] emerged as the most promising precursors for these oxidation reactions. Uemura's precatalyst is generally prepared in situ by mixing Pd(OAc)$_2$ and pyridine (Py) in a 1:2 ratio directly in the reaction medium (i.e., toluene).[5i] Attempts to optimize the efficiency of this precatalyst by varying the molar ratio between Pd(OAc)$_2$ and Py led to the optimized Uemura precatalyst that is characterized by a 1:4 molar ratio between Pd(OAc)$_2$ and Py,[5i] which is the best compromise between optimal turnover rate and catalyst stability with time, as confirmed by Stahl and co-workers' theoretical study on the latter catalytic system.[6]

Since the chemoselective aerobic conversion of unprotected diols into the corresponding hydroxy ketone is important from an atom-economic point of view,[5d,7] we report herein the synthesis, characterization and application of neutral and cationic pyridine-based palladium compounds for the aerobic oxidation of unprotected diols in a 19:1 (v/v) toluene–DMSO solvent mixture.

Results and Discussion

Synthesis and Characterization of Palladium(II) Complexes

Palladium complexes with different palladium-to-ligand ratios have been synthesized and characterized in solution and in the solid state (Scheme 1).

The palladium complexes [Pd(X)(η^3-allyl)(Py)] in which X = OAc (**1a**) and Cl (**2a**) have been obtained by the reaction of [{Pd(X)(η^3-allyl)}$_2$] (X = Cl,[8a] OAc[8b]) with Py in a 1:2 ratio in dichloromethane (Scheme 1, a). Both complexes, which show a dynamic behaviour on the NMR spectroscopic timescale,[5d,9] were obtained as yellowish powders in around 90% yield. The ^{13}C{^{1}H} NMR spectra, acquired at room temperature, showed only one singlet for both allyl-CH_2 groups centred at δ = 57.06 (**1a**) and 61.10 ppm (**2a**), whereas ^{1}H and ^{13}C{^{1}H} NMR spectra acquired at –60 °C showed for both latter compounds well-defined NMR spectroscopic signals for the chemically inequivalent allyl-CH_2

[a] Istituto di Chimica dei Composti Organometallici (ICCOM-CNR),
Area di Ricerca CNR di Firenze, via Madonna del Piano 10, 50019 Sesto Fiorentino, Italy
Fax: +39-055-225-203
E-mail: werner.oberhauser@iccom.cnr.it

Supporting information for this article is available on the WWW under http://dx.doi.org/10.1002/ejic.201001300.

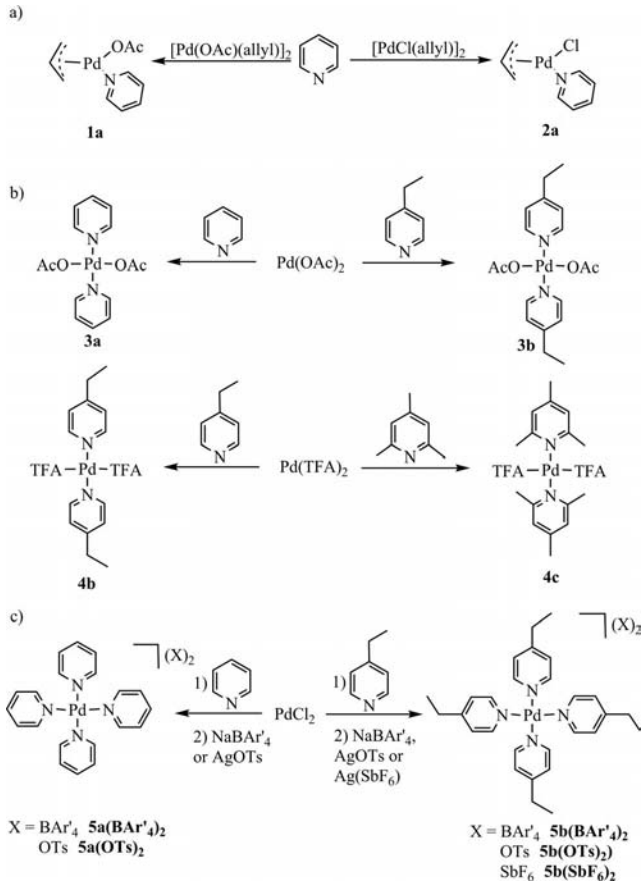

Scheme 1.

groups. Moreover, the ^{13}C cross-polarization (CP) magic angle spinning (MAS) spectra of **1a** and **2a** (Figure S1 in the Supporting Information), which are in agreement with the corresponding $^{13}C\{^1H\}$ NMR spectra in CD_2Cl_2 at –60 °C, and a single-crystal X-ray structure analysis of **2a** confirmed the asymmetric coordination of the η^3-allyl group to palladium in the solid state (Figure S2).

The neutral palladium acetate complexes of the general formula $[Pd(\kappa^1\text{-}O\text{-}OAc)_2(L)_2]$ in which L = Py (**3a**)[10] and 4-EtPy (**3b**) were straightforwardly obtained at room temperature by the reaction of $Pd(OAc)_2$ with the corresponding ligand and applying a 1:2 stoichiometry. Analogously, the neutral palladium–trifluoroacetate complexes of the formula $[Pd(\kappa^1\text{-}O\text{-}tfa)_2(L)_2]$ (tfa = trifluoroacetate) with L = 4-EtPy (**4b**) and 2,4,6-$(Me)_3$Py (**4c**) were obtained by the reaction of $Pd(tfa)_2$ with the corresponding ligand. All these neutral palladium compounds, isolated as yellow or brownish powders in 74 to 80% yield, share a square-planar coordination geometry around palladium with the anionic ligand (i.e., OAc or TFA) located *trans* to each other as confirmed by single-crystal X-ray structure analysis carried out for **3b**, **4b** and **4c** (Figures S3 and S4 in the Supporting Information).

The unsymmetric coordination of 2,4,6-$(Me)_3$Py to palladium in the crystal structure of **4c** is retained in solution. Accordingly, ^1H and $^{13}C\{^1H\}$ NMR spectra of the latter compound acquired in CD_2Cl_2 at room temperature showed for the *ortho*-methyl hydrogen atoms two ^1H NMR spectroscopic singlets centred at δ = 3.71 and 3.72 ppm and two ^{13}C NMR spectroscopic singlets at δ = 24.81 and 25.00 ppm.

The bis-cationic palladium complexes of the type $[Pd(L)_4](X)_2$ {in which L = Py, X = tetra[bis(3,5-trifluoromethyl)-phenyl]borate (BAr'_4) [**5a(BAr'$_4$)$_2$**], OTs [**5a(OTs)$_2$**]; L = 4-EtPy, X = BAr'_4 [**5b(BAr'$_4$)$_2$**], OTs [**5b(OTs)$_2$**], SbF_6 [**5b(SbF$_6$)$_2$**]} were straightforwardly obtained in 85–94% yield by the reaction of $PdCl_2$ with the corresponding ligand in the presence of either $NaBAr'_4$, AgOTs or $Ag(SbF_6)$ as shown in Scheme 1 (c). The structural formulation of these complexes was unambiguously confirmed by integration of the corresponding ^1H NMR spectroscopic signals, by elemental analysis and by a single-crystal structure analysis of **5b(BAr'$_4$)$_2$** and **5b(OTs)$_2$**·$2H_2O$ (Figure 1).

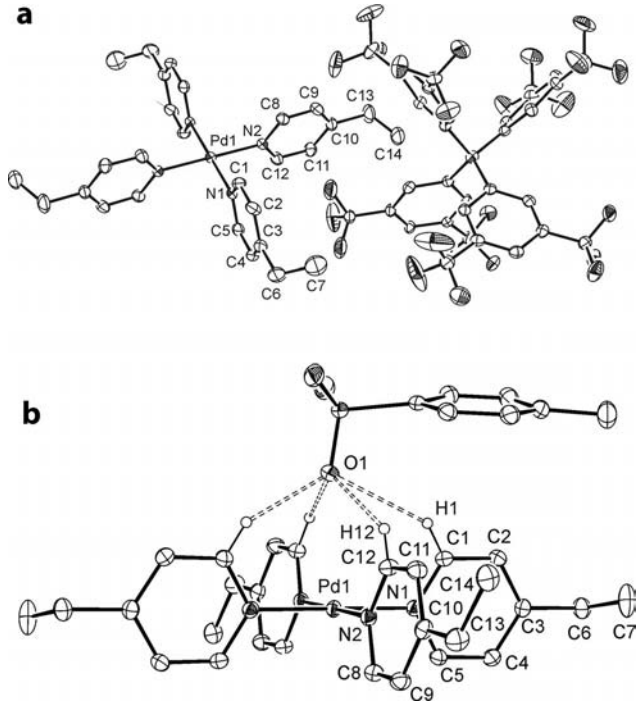

Figure 1. ORTEP plot of **5b(BAr'$_4$)$_2$** (a) and **5b(OTs)$_2$**·$2H_2O$ (b). Thermal ellipsoids are drawn at the 30% probability level and only the asymmetric part of the cations is labelled, whereas the symmetry-related counterion is omitted for clarity. Selected bond lengths [Å] and angles [°] for **5b(BAr'$_4$)$_2$**: Pd1–N1 2.026(3), Pd1–N2 2.020(3), N1–Pd1–N2 90.14(12); for **5b(OTs)$_2$**·$2H_2O$: Pd1–N1 2.021(2), Pd1–N2 2.020(2) and N1–Pd1–N2 90.28(6). Intramolecular distances [Å] for **5b(OTs)$_2$**·$2H_2O$: Pd1···O1 3.096, O1···H1 2.650, O1···H12 2.589.

The crystal structure of **5b(BAr'$_4$)$_2$** and **5b(OTs)$_2$**·$2H_2O$ is centrosymmetric with palladium occupying a centre of inversion. Both molecular structures show an almost perpendicular tilt of the pyridine ring with respect to the metal coordination plane defined by N1, N2 and Pd1 of 80.85(19), 89.57(14)° [**5b(BAr'$_4$)$_2$**] and of 82.92(8), 87.03(10)° [**5b(OTs)$_2$**]. Such a ligand orientation is known for related pyridine-bearing palladium complexes and results from minimizing steric repulsion between the metal-coordinating pyridine ligands.[11] The most important fea-

ture of the latter crystal structures is the different displacement of the counterions with respect to the coordination plane of palladium. Whereas in **5b(BAr′$_4$)$_2$** the anions are located almost in the palladium coordination plane, in **5b(OTs)$_2$**·2H$_2$O both anions are localized symmetry-related above and below the metal coordination plane as shown in Figure 1. As a result, the tosylate oxygen atom O1 and its symmetry-related counterpart occupy axial positions of a pseudo-octahedral metal coordination sphere and show intramolecular distances to Pd1 and to the *ortho*-hydrogen atoms H1 and H12 of 4-EtPy (Figure 1). Similar intramolecular distances between cation and anion have been observed in related palladium complexes that bear weakly coordinating oxygen-donor anions.[11b] ^{1}H NMR spectra of **5a/b(OTs)$_2$** acquired in CD_2Cl_2 or in a 19:1 (v/v) [D$_8$]toluene/[D$_6$]DMSO solvent mixture (i.e., the reaction medium of the aerobic oxidation reactions) showed for the *ortho*-hydrogen atoms of 4-EtPy a significant high-frequency chemical shift of δ = 1.44 ppm relative to **5a/b(BAr′$_4$)$_2$**, thereby proving that the solid-state conformation is retained in solution. Furthermore, conductivity measurements of nitroethane solutions of **5a/b(OTs)$_2$** behave as a 1:1 electrolyte, whereas **5a/b(BAr′$_4$)$_2$** behaves as a 1:2 electrolyte.

To determine the relative σ-electron donor property of the pyridine ligands (i.e., Py, 4-EtPy, 2,4,6-Me$_3$Py) in neutral (i.e., **3a/b**, **4b** and **4c**) and cationic palladium complexes, i.e., **5a/b(BAr′$_4$)**, a CV study was carried out using a 19:1 (v/v) toluene/DMSO solvent mixture (see the Supporting Information). As a result, the cathodic half-wave potential ($E_{½c}$), which is directly correlated to the σ-electron donor property of the Py ligands,[12] increased, as expected, with the increasing σ-electron donation property of the pyridine ligand: Py < 4-EtPy < 2,4,6-(Me)$_3$Py.

Catalytic Study

Compounds **1a**–**5b(SbF$_6$)$_2$** were tested as catalysts for the aerobic oxidation, i.e., air (300 psi) of unprotected 1,2- and 1,3-diols (Scheme 2, **A**–**E**) to give exclusively the corresponding hydroxy ketones (Scheme 2, **A′**–**E′**) in a 19:1 (v/v) toluene/DMSO mixture, which solubilizes all substrates employed in this study. Catalytic reactions carried out in other organic solvents such as THF and CH_3CN led to much lower substrate conversion. The catalytic reactions were carried out either in the presence or in the absence of an external base, i.e., K_2CO_3. The substitution of K_2CO_3 by either Na_2CO_3 or Cs_2CO_3 gave no benefit in terms of substrate conversion or catalyst stability with time.

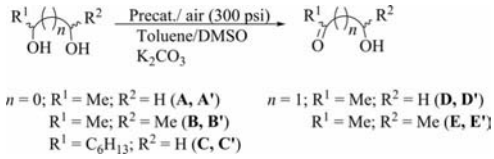

Scheme 2.

The catalytic activity of **1a–5b(SbF$_6$)$_2$** was screened by employing 1,2-propanediol as test substrate, and the results of this comparative catalytic study are compiled in Table 1.

Regardless of the precursor employed for the aerobic oxidation of 1,2-propanediol, hydroxyacetone was chemoselectively obtained. The catalyst derived from **3a** converted 46% of 1,2-propanediol to hydroxyacetone after 1 h reaction time (Table 1, entry 4). An analogous reaction in the presence of 2 mol-equiv. of K_2CO_3 showed only a slight increase of substrate conversion (Table 1, entry 4 vs. 5). This experimental result confirms the efficiency of acetate as internal base. A comparison of the catalytic activity of **3a**

Table 1. Aerobic oxidation of 1,2-propanediol catalyzed by **1a**–**5b(SbF$_6$)$_2$**.

Entry[a]	Precursor	K_2CO_3 [mol-equiv.]	Conversion [%][b]		
			0.5 h	1 h	2 h
1	**1a**	–	40	41	–
2	**1a**	2	38	51	52
3	**2a**	2	37	47	50
4	**3a**	–	40	46	48
5	**3a**	2	38	49	59
6	**3b**	–	–	50	62
7	**3b**	2	–	53	73
8	**3b**	4	–	48	63
9[c]	**3b**	–	–	34	72
10	**4b**	–	–	11	12
11	**4b**	2	–	65	80
12	**4c**	2	–	56	67
13	**5a(BAr′$_4$)$_2$**	2	–	19	30
14	**5a(OTs)$_2$**	2	–	55	69
15	**5b(BAr′$_4$)$_2$**	2	–	29	36
16	**5b(OTs)$_2$**	–	–	1.1	2.1
17	**5b(OTs)$_2$**	2	46	80	90
18	**5b(OTs)$_2$**	4	–	61	74
19	**5b(SbF$_6$)$_2$**	2	–	60	79

[a] Catalytic conditions: catalyst precursor (0.01 mmol), 1,2-propanediol (1.00 mmol), 19:1(v/v) toluene/DMSO (20 mL), 80 °C, *p*(air) (300 psi), mol-equiv. of K_2CO_3 with respect to the amount of catalyst precursor. [b] Conversion given as average value of 3 runs using decane as internal standard for GC analysis. [c] Addition of 4-EtPy (0.02 mmol).

with that of **1a**, which bears only one coordinated acetate and one pyridine ligand, shows an identical substrate conversion for a short reaction time (i.e., 0.5 h; Table 1, entries 4 and 5 vs. 1 and 2). In this context, it is important to mention that **1a** enters the catalytic cycle by a substrate-mediated protonation of the coordinated allyl moiety,[5d] thereby resulting in a Pd–alkoxy species under the concomitant release of propene, the presence of which in the catalytic solution has been proven by ^{1}H NMR spectroscopy and GC–MS analysis. To underscore the fact that acetate in **1a** does not function as an internal base, an identical catalytic reaction with **2a**, which contains chloride instead of acetate (Table 1, entry 3 vs. 2), was carried out and gave almost identical substrate conversion.

The increasing substrate conversion in the presence of K_2CO_3 obtained either by substituting Py in **3a** for the stronger σ-electron-donating 4-EtPy (**3b**) or by substituting OAc in **3b** for TFA (**4b**) confirms that the observed catalytic activity is the result of the easier anion dissociation (i.e., TFA vs. OAc) and the stabilization of the catalytic species by a stronger σ-electron donor (i.e., 4-EtPy vs. Py). It is worth mentioning that neutral palladium complexes that contain a weaker base than OAc, such as TFA or chloride, need an external base to be converted into the catalytically active Pd–alkoxy species.[7] Further increasing the σ-electron donor property of the pyridine ligand by using 2,4,6-Me_3Py (**4c**) clearly showed that a more reluctant ligand dissociation from the precursor molecule results in a decrease of the catalytic activity observed for **4c** relative to **4b** (Table 1, entry 12 vs. 11).

In accordance with Uemura's optimized precatalyst, the contemporary presence of **3b** and 4-EtPy (2 mol-equiv.) in the catalytic solution [i.e., **3b/2(4-EtPy)**], which does not lead to the formation of a bis-cationic palladium complex of the formula $[Pd(4\text{-}EtPy)_4](OAc)_2$, as proven by ^{1}H NMR spectroscopy, led to an increased catalyst stability with time relative to **3b** (Table 1, entry 9 vs. 6).

Within the series of bis-cationic palladium precursors investigated for the aerobic oxidation of unprotected diols, **5b(OTs)$_2$** in conjunction with external base (2 mol-equiv. of, i.e., K_2CO_3) has emerged as the most active catalyst precursor and outperforms **3b/2(4-EtPy)** under comparable catalytic conditions (Table 1, entry 17 vs. 9). It is important to mention that the bis-cationic precursors need the presence of an external base to enter the catalytic cycle. In this respect, 2 mol-equiv. of base (in reference to the amount of precursor) is the optimal amount (Table 1, entry 17 vs. 16 and 18).

A comparison of the catalytic performance of **5b(OTs)$_2$** and **5b(SbF$_6$)$_2$** with that of **5b(BAr′$_4$)$_2$** clearly showed the presence of an anion effect on the catalytic performance of the bis-cationic precursors. Indeed, within the series of bis-cationic catalyst precursors, the tosylate precursor showed the highest and the BAr'_4 counterpart the lowest catalytic activity (Table 1, entry 17 vs. 15 and 19).

Since **5b(OTs)$_2$** in combination with 2 mol-equiv. of K_2CO_3 was the most promising precursor, its application was extended to other diols such as 2*R*,3*R*-butanediol (B), 1,2-octanediol (C), (±)-1,3-butanediol (D) and a 1:1 mixture of *meso*-/*rac*-2,4-pentanediol (E) (Scheme 2). The catalytic performance of **5b(OTs)$_2$** was compared with that of **3b/2(4-EtPy)** with which it shares a Pd^{II}-to-ligand ratio of 1:4. The results of the comparative catalytic study are listed in Table 2.

Table 2. Aerobic oxidation of diols catalyzed by **3b/2(4-EtPy)** and **5b(OTs)$_2$**.

Entry[a]	Precursor	Substrate	Conversion [%][b]	
			1 h (TOF)[c]	2 h (TOF/Yield)[c]
1	**3b/2(4-EtPy)**	A	34	72
2[d]	**5b(OTs)$_2$**	A	80(80)	90(45)
3[d,e]	**5b(OTs)$_2$**	A	30(120)	45(90/43)
4	**3b/2(4-EtPy)**	B	37	57
5[d]	**5b(OTs)$_2$**	B	71(71)	95(47)
6[d,e]	**5b(OTs)$_2$**	B	25(100)	37(74/34)
7	**3b/2(4-EtPy)**	C	30	55
8[d]	**5b(OTs)$_2$**	C	80(80)	95(95)
9[d,e]	**5b(OTs)$_2$**	C	35(140)	55(110/53)
10	**3b/2(4-EtPy)**	D	46	56
11[d]	**5b(OTs)$_2$**	D	65	84
12	**5b/2(4-EtPy)**	E	45	49
13[d]	**5b(OTs)$_2$**	E	59	75

[a] Catalytic conditions: catalyst precursor (0.01 mmol), substrate (1.00 mmol), 19:1 (v/v) toluene/DMSO (20 mL), *p*(air) 300 psi, 80 °C. [b] Conversion given as average value of 3 runs using decane as internal standard for GC analysis. [c] Turnover frequency (TOF) values are expressed as (mmol substrate) × [(mmol Pd) × hour]$^{-1}$; isolated yield given in %. [d] Addition of K_2CO_3 (0.02 mmol). [e] Substrate (4.00 mmol).

Both catalyst precursors chemoselectively converted the diols into the corresponding hydroxy ketones as shown in Scheme 2. A perusal of Table 2 shows **5b(OTs)$_2$** to be more efficient than **3b/2(4-EtPy)**, regardless of the substrate employed. The catalytic performance of the former catalyst precursor was particularly pronounced with 1,2-diols and showed for a substrate-to-precursor ratio of 400 a TOF of up to 140 (Table 2, entry 9). On the other hand, using 1,3-diols instead of 1,2-diols caused a drop of the catalytic activity of **5b(OTs)$_2$** as is evident from the results compiled in Table 2.

Operando ^{1}H HPNMR Spectroscopic Study

In an attempt to spectroscopically follow the **5b(OTs)$_2$**-catalyzed aerobic oxidation reaction of 1,2-propanediol, an operando HPNMR experiment was carried out in a [D_8]-toluene/[D_6]DMSO (19:1 v/v) solvent mixture. This catalytic reaction was followed by variable-temperature ^{1}H NMR spectroscopy and selected ^{1}H NMR spectra in the pertinent chemical-shift range from δ = 6.4 to 10.4 ppm are shown in Figure 2.

The ^{1}H NMR spectrum of a 19:1 (v/v) [D_8]toluene/[D_6]DMSO solution of **5b(OTs)$_2$** showed for the *ortho*-hydrogen atoms of 4-EtPy a high-frequency doublet at δ = 10.25 ppm ($^3J_{H,H}$ = 8.8 Hz) (Figure 2, trace a). An analogous spectrum of **5b(BAr′$_4$)$_2$** under identical experimental conditions showed for the same hydrogen atoms a doublet centred at δ = 9.18 ppm. This spectroscopic finding is in-

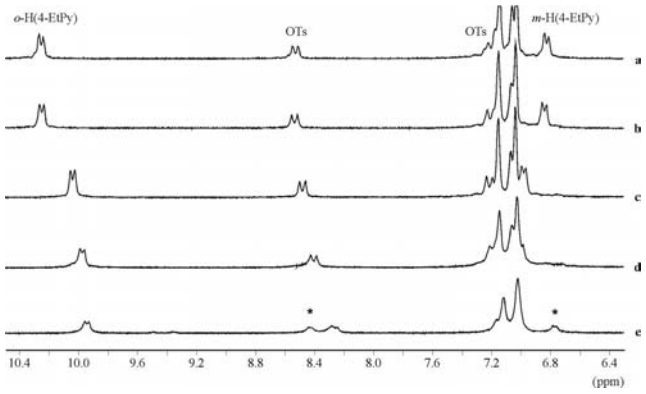

Figure 2. Variable-temperature ^{1}H HPNMR spectroscopic study of the aerobic oxidation of 1,2-propanediol with **5b(OTs)$_2$** [sapphire tube, 19:1 (v/v) [D$_8$]toluene/[D$_6$]DMSO, 200.13 MHz, δ values (ppm)]: (a) **5b(OTs)$_2$** at room temperature; (b) addition of K_2CO_3 (2 mol-equiv.); (c) addition of 1,2-propanediol (50 μL); (d) after charging with air (300 psi) at room temperature; and (e) after 1 h at 80 °C. Asterisks denote signals of uncoordinated 4-EtPy.

dicative of a hydrogen-bond-based interaction between OTs and the *ortho*-hydrogen atoms of the metal-coordinated 4-EtPy. The addition of K_2CO_3 (2 mol-equiv.) to the latter solution did not change the NMR spectroscopic pattern (trace b), whereas by addition of 1,2-propanediol to the latter solution, the ^{1}H NMR spectroscopic doublet assigned to the *ortho*-hydrogen atoms of 4-EtPy shifted to 10.03 ppm and also the ^{1}H NMR spectroscopic doublet assigned to OTs shifted to slightly lower frequency (trace c). This evidence is indicative of adduct formation between 1,2-propanediol and the *ortho*-hydrogen atoms of 4-EtPy, which is similar to that reported by Stahl et al. between **3a** and benzyl alcohol.[6] In fact, an adduct formation between the substrate and the catalyst precursor is a prerequisite for a substrate-induced substitution reaction of 2-EtPy. By charging the sapphire tube with air (300 psi) at room temperature no alteration of the ^{1}H NMR spectroscopic pattern occurred (trace d), whereas on heating the sapphire tube to 80 °C for 1 h, two new broad ^{1}H NMR spectroscopic doublets centred at δ = 8.56 and 6.75 ppm appeared in the corresponding NMR spectrum (trace e). These ^{1}H NMR spectroscopic doublets were safely attributed to uncoordinated 4-EtPy, due to the formation of Pd^0 in the course of the catalytic oxidation reaction. It is important to mention at this point that **5b(OTs)$_2$** is stable in [D$_8$]toluene/[D$_6$]DMSO even upon heating the latter solution at 80 °C, as proven by ^{1}H NMR spectroscopy.

Based on batch catalytic reactions and HPNMR spectroscopic experiments, we propose for the aerobic oxidation of diols mediated by bis-cationic Pd–pyridine-based catalysts a catalytic cycle as shown in Scheme 3.

The bis-cationic Pd^{II}-based catalyst precursors (**5**) are converted into the catalytically active monocationic Pd–alkoxy species (**7**) by removing two pyridine ligands from the metal centre and the successive deprotonation reaction of the coordinated substrate by an external base (i.e., K_2CO_3) (Scheme 3). The substrate-mediated ligand-substitution reaction is most likely an equilibrium reaction. The extent to which this latter equilibrium is shifted to the substrate-coordinated species depends on: (i) the "bite angle" of the diol employed (i.e., 1,2-diols more favoured than 1,3-diols; Table 2); (ii) the bulkiness of the counterion of the catalytic precursor involved, as experimentally proven by a comparison of the catalytic activity of **5b(BAr′$_4$)$_2$**, **5b(SbF$_6$)$_2$** and **5b(OTs)$_2$** (Table 1). In this context, the single-crystal X-ray structure analysis of **5b(BAr′$_4$)$_2$** clearly shows the localization of the counterions in the coordination plane of palladium, which contrasts with the crystal structure of **5b(OTs)$_2$**·2H$_2$O (vide infra). In addition, the experimental fact that **5b(OTs)$_2$** showed a higher catalytic activity when compared to **5b(SbF$_6$)$_2$** (Table 1) might be ascribed to the stabilizing effect of OTs through coordination to palladium (Scheme 3) fostering the oxygen insertion into the Pd^{II}–hydride bond due to its hydrogen-bond acceptor property.[13]

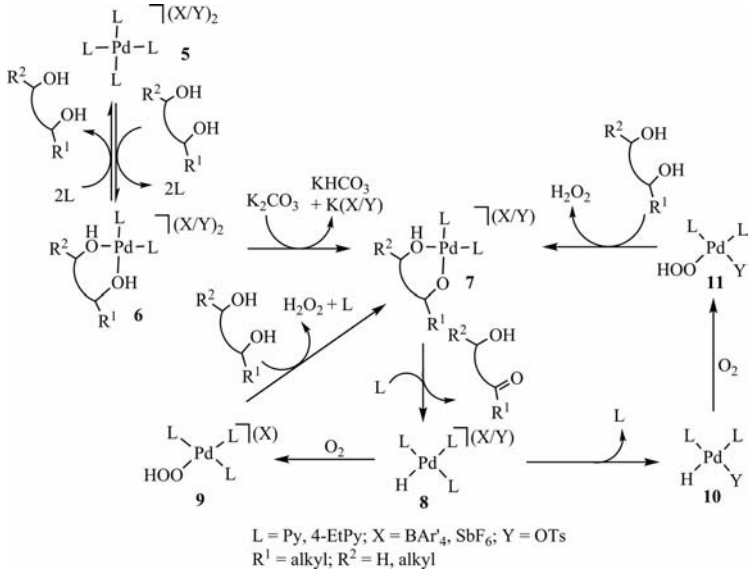

Scheme 3. Proposed catalytic cycle for the chemoselective aerobic oxidation of unprotected diols by cationic Pd–pyridine-based catalysts.

Monocationic Pd^{II}–alkoxy species **7** undergoes a β-hydride elimination reaction to give monocationic Pd^{II}–hydride **8** under the concomitant release of hydroxy ketone. Then, **8** inserts oxygen to yield Pd–hydroperoxide species **9**. The catalytic cycle is then closed by the reaction of the substrate with **9** to release H_2O_2. The presence of H_2O_2 in the catalytic solution has been proven upon interception of dimethylsulfone by GC analysis of the catalytic solution. Importantly, the oxidation of DMSO to dimethylsulfone by H_2O_2 has been proven by carrying out a blank reaction.[5d]

The most significant differences between the bis-cationic Pd–pyridine- and the **3b/2(4-EtPy)**-based catalytic cycle (Scheme 4) can be summarized as follows: (i) unlike the bis-cationic Pd precursors, **3b/2(4-EtPy)** enters the catalytic cycle by an intramolecular reaction of one coordinated acetate molecule with the substrate, whereas the second acetate molecule remains coordinated to palladium throughout the catalytic cycle (Scheme 4); (ii) the Pd–alkoxy species formed from **3b/2(4-EtPy)** is neutral and may thus undergo a much slower β-hydride elimination reaction compared to the monocationic counterpart formed from bis-cationic Pd precursors (Scheme 3); and (iii) the Pd–hydroperoxy species in the **3b/2(4-EtPy)**-based catalytic cycle can alternatively be formed by an aerobic, acetate-mediated oxidation of Pd^0 (Scheme 4).[5a,14]

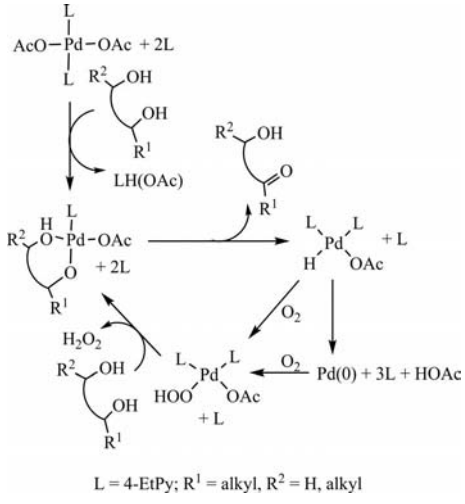

Scheme 4. Proposed catalytic cycle for the chemoselective aerobic oxidation of unprotected diols by **3b/2(4-EtPy)**.

Conclusion

A series of neutral and cationic pyridine-based palladium complexes have been synthesized, completely characterized and tested as catalyst precursors for the aerobic oxidation of unprotected diols to chemoselectively yield the corresponding hydroxy ketone. The comparative catalytic study showed that the bis-cationic precursor **5b(OTs)$_2$** in combination with an external base (i.e., K_2CO_3) outperforms the neutral optimized Uemura-type precatalyst **3b/2(4-EtPy)**. The efficiency of bis-cationic catalyst precursors in the aerobic oxidation of unprotected diols has been found to depend on (i) the coordination property of the diol employed to Pd^{II} (i.e., 1,2-diols show higher conversion than 1,3-diols); and (ii) the bulkiness and coordination property of the counterion (i.e., the OTs precursor showed the highest and the BAr'_4 counterpart the lowest catalytic activity).

Experimental Section

General Procedure: All synthetic reactions were carried out in air by using round-bottomed flasks. Solvents were either distilled or passed through columns that contained dehydrating agents. Reagents were used as received from Aldrich unless stated otherwise. Compounds $[PdCl(\eta^3\text{-allyl})]_2$,[8a] $[Pd(\kappa^2\text{-O-OAc})(\eta^3\text{-allyl})]_2$[8b] and **3a**[10] were prepared according to literature methods. Deuterated solvents for routine NMR spectroscopic measurements were dried with activated molecular sieves. ^1H and $^{13}C\{^1H\}$ NMR spectra were obtained with a Bruker Avance DRX-400 spectrometer acquiring spectra at 400.13 and 100.62 MHz, respectively. Chemical shifts are reported in ppm (δ) with reference to TMS as an internal standard (^1H and $^{13}C\{^1H\}$ NMR spectra). ^1H HPNMR spectroscopic experiments were carried out with a Bruker Avance II-200 spectrometer equipped with a 10 mm BB probe using a 10 mm sapphire tube [Saphikon (Milford, NH), equipped with a titanium high-pressure charging head constructed at ICCOM-CNR].[15] CP-MAS ^{13}C NMR spectra were acquired with a Bruker Avance DRX-400 spectrometer equipped with a 4 mm BB CP-MAS probe at a working frequency of 100.62 MHz and a spinning rate of 10 kHz. Microanalyses were performed with a Carlo–Erba Model 1106 elemental analyzer. Conductivities were measured with an ORION Model 990101 conductance cell connected to a conductivity meter. The conductivity data were obtained at sample concentrations of around 0.001 M in nitroethane.[16] Oxidation reactions were performed with 65 mL stainless steel autoclaves, constructed at ICCOM-CNR, equipped with magnetic stirring, oil-bath heating and a temperature and pressure controller. GC analyses were performed with a Shimadzu 2010 gas chromatograph equipped with a flame ionization detector and a 30 m (0.25 mm i.d., 0.25 μm film thickness) VF-WAXms capillary column. Decane was used as internal standard. GC–MS analyses were performed with a Shimadzu QP 5000 apparatus, equipped with a 30 m (0.32 mm i.d., 0.50 μm film thickness) CP-WAX 52 CB WCOT-fused silica column.

Synthesis of 1a: $[\{Pd(\kappa^2\text{-}O\text{-OAc})(\eta^3\text{-allyl})\}_2]$ (350.0 mg, 0.848 mmol) was dissolved in CH_2Cl_2 (10 mL). Py (167.0 μL, 2.050 mmol) was added to this solution under vigorous stirring at room temperature. The resulting solution was allowed to stir at room temperature for 1 h. Afterwards, the solution was concentrated to a small volume (2 mL) and on addition of diethyl ether (15.0 mL) the product precipitated as brownish powder that was separated by filtration and washed with diethyl ether (3×5 mL). The solid was then dried in a stream of nitrogen; yield 445.5 mg (92%). $C_{10}H_{13}NO_2Pd$ (285.51): calcd. C 42.07, H 4.55, N 4.90; found C 41.95, H 4.40, N 4.73. ^1H NMR (400.13 MHz, CD_2Cl_2, 21 °C): δ = 1.95 (s, 3 H, CH_3CO_2), 3.15 (d, $^3J_{H,H}$ = 11.6 Hz 2 H, allyl-C_aH_2), 3.87 (br. s, 2 H, allyl-C_bH_2), 5.62 (quintet, $^3J_{H,H}$ = 6.4 Hz, 1 H, allyl-CH), 7.43 (m, 2 H, *m*-Ar–H), 7.86 (m, 1 H, *p*-Ar–H), 8.69 (m, 2 H, *o*-Ar–H) ppm. $^{13}C\{^1H\}$ NMR (100.62 MHz, CD_2Cl_2, 21 °C): δ = 23.60 (s, CH_3CO_2), 57.06 (br. s, allyl-CH_2), 113.51 (s, allyl-CH), 124.99 (s, Ar–C), 137.90 (s, Ar–C), 151.91 (s, Ar–C), 176.00 (br. s, CH_3CO_2) ppm. ^1H NMR (400.13 MHz, CD_2Cl_2, –60 °C): δ = 1.93 (s, 3 H, CH_3CO_2), 2.96 (d, $^3J_{H,H}$ = 11.6 Hz, 1 H, allyl-C_aHH'), 3.07 (d, $^3J_{H,H}$ = 12.4 Hz, 1 H, allyl-C_bHH'), 3.67 (d, $^3J_{H,H}$ = 6.8 Hz, 1 H, allyl-C_aHH'), 3.96 (d, $^3J_{H,H}$

= 6.8 Hz, 1 H, allyl-C_bHH'), 5.64 (quintet, $^3J_{H,H}$ = 6.0 Hz, 1 H, allyl-CH), 7.43 (m, 2 H, *m*-Ar–H), 7.87 (m, 1 H, *p*-Ar–H), 8.59 (m, 2 H, *o*-Ar–H) ppm. $^{13}C\{^1H\}$ NMR (100.62 MHz, CD_2Cl_2, –60 °C): δ = 24.10 (s, CH_3CO_2), 57.39 (s, allyl-C_aHH'), 58.00 (s. allyl-C_bHH'), 114.52 (s, allyl-CH), 125.51 (s, Ar-C), 138.51 (s, Ar–C), 152.10 (s, Ar–C), 177.18 (s, CH_3CO_2) ppm. CP-MAS ^{13}C NMR: δ = 28.30 (s, CH_3CO_2), 60.30 (s, allyl-C_aHH', C_bHH'), 113.20 (s, allyl-CH), 128.20 (s, Ar–C), 139.10 (s, Ar–C), 153.20 (s, Ar–C), 178.10 (s, CH_3CO_2) ppm.

Synthesis of 2a: [{Pd(Cl)(η^3-allyl)}$_2$] (310.2 mg, 0.848 mmol) was dissolved in CH_2Cl_2 (10 mL). Py (167.0 μL, 2.050 mmol) was added to this solution under vigorous stirring at room temperature. The obtained yellow solution was allowed to stir at the same temperature for 1 h, followed by its concentration to a small volume (2 mL). Addition of diethyl ether (10 mL) caused the precipitation of the product as yellow powder that was separated by filtration washed with diethyl ether (3 × 5 mL) and dried in a stream of nitrogen; yield 399.8 mg (90%). $C_8H_{10}ClNPd$ (261.96): calcd. C 36.68, H 3.82, N 5.34; found C 36.81, H 3.90, N 5.15. ^1H NMR (400.13 MHz, CD_2Cl_2, 21 °C): δ = 3.13 (d, $^3J_{H,H}$ = 12.2 Hz, 2 H, allyl-C_aHH'), 4.04 (d, $^3J_{H,H}$ = 6.8 Hz, 2 H, allyl-C_bHH'), 5.67 (m, 2 H, allyl-CH), 7.45 (m, 2 H, *m*-Ar–H), 7.87 (m, 1 H, *p*-Ar–H), 8.84 (m, 2 H, *o*-Ar–H) ppm. $^{13}C\{^1H\}$ NMR (100.62 MHz, CD_2Cl_2, 21 °C): δ = 61.10 (br. s, allyl-CH_2), 114.23 (s, allyl-CH), 125.02 (s, Ar–C), 137.99 (s, Ar–C), 152.54 (s, Ar–C) ppm. ^1H NMR (400.13 MHz, CD_2Cl_2, –60 °C): δ = 2.98 (d, $^3J_{H,H}$ = 12.4 Hz, 1 H, allyl-C_aH*H'*), 3.24 (d, $^3J_{H,H}$ = 12.4 Hz, 1 H, allyl-C_bH*H'*), 3.95 (d, $^3J_{H,H}$ = 6.8 Hz, 1 H, allyl-C_a*H*H'), 4.03 (d, $^3J_{H,H}$ = 5.6 Hz, 1 H, allyl-C_b*H*H'), 5.67 (m, 1 H, allyl-CH), 7.44 (m, 2 H, *m*-Ar–H), 7.87 (m, 1 H, *p*-Ar–H), 8.75 (m, 2 H, *o*-Ar–H) ppm. $^{13}C\{^1H\}$ NMR (100.62 MHz, CD_2Cl_2, –60 °C): δ = 58.07 (s, allyl-C_aHH'), 64.74 (s. allyl-C_bHH'), 114.99 (s, allyl-CH), 125.40 (s, Ar–C), 138.45 (s, Ar–C), 152.60 (s, Ar–C) ppm. CP-MAS ^{13}C NMR: δ = 58.10 (br. s, allyl-C_aHH'), 68.31 (s, allyl-C_bHH'), 118.40 (s, allyl-CH), 125.40 (s, Ar–C), 138.21 (s, Ar–C), 153.80 (s, Ar–C) ppm.

Synthesis of 3b: $Pd(OAc)_2$ (119.9 mg, 0.534 mmol) was dissolved in CH_2Cl_2 (8 mL). Afterwards, 4-EtPy (124 μL, 1.070 mmol) was added to the solution and stirred for 1 h. The latter solution was then concentrated to a small volume (2 mL) by means of vacuum and on addition of diethyl ether (10.0 mL) the product was precipitated as light brown powder that was separated by filtration, washed with diethyl ether (3 × 5 mL) and dried in a stream of nitrogen; yield 175.6 mg (75%). $C_{18}H_{24}N_2O_4Pd$ (438.61): calcd. C 49.29, H 5.47, N 6.38; found C 49.19, H 5.39, N 6.30. ^1H NMR (400.13 MHz, CD_2Cl_2, 21 °C): δ = 1.27 (t, $^3J_{H,H}$ = 8.0 Hz, 6 H, CH_3CH_2), 1.83 (s, 6 H, CH_3CO_2), 2.72 (q, $^3J_{H,H}$ = 8.0 Hz, 4 H, CH_3CH_2), 7.22 (d, $^3J_{H,H}$ = 6.4 Hz, 4 H, *m*-Ar–H), 8.46 (d, $^3J_{H,H}$ = 6.4 Hz, 4 H, *o*-Ar–H) ppm. $^{13}C\{^1H\}$ NMR (100.62 MHz, CD_2Cl_2, 21 °C): δ = 13.63 (s, CH_3CH_2), 22.95 (s, CH_3CO_2) 28.08 (s, CH_3CH_2), 124.51 (s, *m*-Ar–C), 150.71 (s, *o*-Ar–C), 156.62 (s, *p*-Ar–C), 177.51 (s, CH_3CO_2) ppm.

Synthesis of 4b: $Pd(TFA)_2$ (197.9 mg, 0.595 mmol) was dissolved in CH_2Cl_2 (10 mL), followed by the addition of 4-EtPy (130 μL, 1.190 mmol). The obtained solution was allowed to stir at room temperature for 1 h. Afterwards the solvent was completely removed by vacuum and the obtained solid was suspended in diethyl ether (10 mL). The brownish powder was separated from solution by filtration, washed with diethyl ether (3 × 5 mL) and dried in a stream of nitrogen; yield 260.1 mg (80%). $C_{18}H_{18}F_6N_2O_4Pd$ (546.60): calcd. C 39.55, H 3.29, N 5.12; found C 39.48, H 3.20, N 5.01. ^1H NMR (400.13 MHz, CD_2Cl_2, 21 °C): δ = 1.28 (t, $^3J_{H,H}$ = 7.8 Hz, 6 H, CH_3CH_2), 2.75 (q, $^3J_{H,H}$ = 7.8 Hz, 4 H, CH_3CH_2), 7.28 (d, $^3J_{H,H}$ = 8.0 Hz, 4 H, *m*-Ar–H), 8.36 (d, $^3J_{H,H}$ = 8.0 Hz, 4 H, *o*-Ar–H) ppm. $^{13}C\{^1H\}$ NMR (100.62 MHz, CD_2Cl_2, 21 °C): δ = 13.50 (s, CH_3CH_2), 28.08 (s, CH_3CH_2), 113.98 (q, $^1J_{C,F}$ = 289.9 Hz, CF_3CO_2), 125.10 (s, *m*-Ar–C), 150.06 (s, *o*-Ar–C), 157.92 (s, *p*-Ar–C), 162.22 (q, $^2J_{C,F}$ = 36.2 Hz, CF_3CO_2) ppm.

Synthesis of 4c: $Pd(TFA)_2$ (179.4 mg, 0.540 mmol) was dissolved in CH_2Cl_2 (8 mL). 2,4,6-Me_3Py (144.0 μL, 1.079 mmol) was added to this solution. The obtained solution was allowed to stir at room temperature for 1 h, followed by its concentration to a small volume (2 mL). On addition of diethyl ether the product precipitated as yellow-brownish powder that was separated by filtration, washed with diethyl ether and then dried in a stream of nitrogen; yield 229.6 mg (74%). $C_{20}H_{22}F_6N_2O_4Pd$ (574.62): calcd. C 41.80, H 3.83, N 4.87; found C 41.72, H 3.78, N 4.80. ^1H NMR (400.13 MHz, CD_2Cl_2, 21 °C): δ = 2.33 (s, 6 H, *p*-CH_3), 3.71 (s, 6 H, *o*-CH_3), 3.72 (s, 6 H, *o*-CH_3), 6.94 (s, 2 H, *m*-Ar–H), 6.97 (s, 2 H, *m*-Ar–H) ppm. $^{13}C\{^1H\}$ NMR (100.62 MHz, CD_2Cl_2, 21 °C): δ = 20.38 (s, *p*-CH_3), 24.81 (s, *o*-CH_3), 25.00 (s, *o*-CH_3), 113.54 (q, $^1J_{C,F}$ = 290.0 Hz, CF_3CO_2), 123.75 (s, *m*-Ar–C), 124.24 (s, *m*-Ar–C), 151.75 (s, *p*-Ar–C), 160.52 (s, *o*-Ar–C), 160.76 (s, *o*-Ar–C), 162.16 (q, $^2J_{C,F}$ = 36.6 Hz, CF_3CO_2) ppm.

Synthesis of 5a(BAr′$_4$)$_2$ and 5a(OTs)$_2$: $PdCl_2$ (56.4 mg, 0.318 mmol) was suspended in CH_2Cl_2 (10 mL). Py (109.0 μL, 1.332 mmol) was added to this latter suspension and the obtained yellow solution was allowed to stir for 1 h. Afterwards, NaBAr′$_4$ (567.2 mg, 0.640 mmol) or AgOTs (178.6 mg, 0.640 mmol) was added to the solution, which caused the precipitation of NaCl and AgCl, respectively. The obtained suspension was allowed to stir in the dark at room temperature for 1 h, followed by its filtration through a plug of celite. The obtained solution was then concentrated to dryness. **5a(BAr′$_4$)$_2$**: Yield 580.8 mg (85%). $C_{84}H_{44}B_2F_{48}N_4Pd$ (2148.86): calcd. C 46.95, H 2.05, N 2.60; found C 46.80, H 1.98, N 2.45. **5a(OTs)$_2$**: Yield 210.9 mg (90%). $C_{34}H_{34}N_4O_6PdS_2$ (764.91): calcd. C 53.39, H 4.44, N 7.32; found C 53.20, H 4.50, N 7.20.

NMR Spectroscopic Data for 5a(BAr′$_4$)$_2$: ^1H NMR (400.13 MHz, CD_2Cl_2, 21 °C): δ = 7.35 [dd, $^3J_{H,H}$ = 8.0, $^3J_{H,H}$ = 6.4 Hz, 8 H, *m*-Ar–H(Py)], 7.59 [s, 8 H, *p*-Ar–H(BAr′$_4$)], 7.76 [br. s, 16 H, *o*-Ar–H(BAr′$_4$)], 8.01 [tt, $^3J_{H,H}$ = 8.0, $^4J_{H,H}$ = 1.2 Hz, 4 H, *p*-Ar–H(Py)], 8.32 [dd, $^3J_{H,H}$ = 6.4, $^4J_{H,H}$ = 1.2 Hz, 8 H, *o*-Ar–H(Py)] ppm. $^{13}C\{^1H\}$ NMR (100.62 MHz, CD_2Cl_2, 21 °C): δ = 117.52 [s, *p*-Ar–C(BAr′$_4$)], 124.54 (q, $^1J_{C,F}$ = 272.5 Hz, CF_3C), 128.81 [s, *m*-Ar–C(Py)], 129.99 [q, $^2J_{C,F}$ = 38.7 Hz, *m*-Ar–C(BAr′$_4$)], 134.77 [s, *o*-Ar–C(BAr′$_4$)], 142.78 [s, *p*-Ar–C(Py)], 150.14 [s, *o*-Ar–C(Py)], 161.72 [m, *ipso*-Ar–C(BAr′$_4$)] ppm. This complex behaves as an 1:2 electrolyte in nitroethane (Λ_M = 113 Ω^{-1} cm^2 mol^{-1}).[16]

NMR Spectroscopic Data for 5a(OTs)$_2$: ^1H NMR (400.13 MHz, CD_2Cl_2, 21 °C): δ = 2.43 (s, 6 H, CH_3), 7.29 [d, $^3J_{H,H}$ = 6.4 Hz, 4 H, Ar–H(OTs)], 7.37 [dd, $^3J_{H,H}$ = 7.6 , $^3J_{H,H}$ = 6.4 Hz, 8 H, *m*-Ar–H(Py)], 7.75 [tt, $^3J_{H,H}$ = 7.6, $^4J_{H,H}$ = 1.2 Hz, 4 H, *p*-Ar–H(Py)], 7.99 [d, $^3J_{H,H}$ = 6.4 Hz, 4 H, Ar–H(OTs)], 9.76 [dd, $^3J_{H,H}$ = 6.4, $^4J_{H,H}$ = 1.2 Hz, 8 H, *o*-Ar–H(Py)] ppm. $^{13}C\{^1H\}$ NMR (100.62 MHz, CD_2Cl_2, 21 °C): δ = 21.04 (s, CH_3), 125.98 [s, *m*-Ar–C(Py)], 126.43 [s, Ar–C(OTs)], 128.60 [s, Ar–C(OTs)], 139.33 [s, *p*-Ar–C(Py)], 139.54 [s, Ar–C(OTs)], 144.62 [s, Ar–C(OTs)], 152.36 [s, *o*-Ar–C(Py)] ppm. This complex behaves as an 1:1 electrolyte in nitroethane (Λ_M = 58 Ω^{-1} cm^2 mol^{-1}).[16]

Synthesis of 5b(BAr′$_4$)$_2$, 5b(OTs)$_2$ and 5b(SbF$_6$)$_2$: $PdCl_2$ (53.0 mg, 0.299 mmol) was suspended in CH_2Cl_2 (10 mL), followed by the addition of 4-EtPy (139.5 μL, 1.226 mmol) and the obtained solution was allowed to stir for 1 h. Afterwards, NaBAr′$_4$ (556.5 mg, 0.628 mmol), AgOTs (175.2 mg, 0.628 mmol) or Ag(SbF_6) (215.8 mg, 0.628 mmol) was added to the solution, which caused

the precipitation of NaCl and AgCl, respectively. The obtained suspension was allowed to stir in the dark at room temperature for 1 h. The suspension was then filtered through a plug of celite and the obtained solution was concentrated to dryness. **5b(BAr′$_4$)$_2$**: Yield 608.3 mg (90%). $C_{92}H_{60}B_2F_{48}N_4Pd$ (2260.95): calcd. C 48.87, H 2.65, N 2.48; found C 48.77, H 2.55, N 2.30. **5b(OTs)$_2$**: Yield 246.5 mg (94%). $C_{42}H_{50}N_4O_6PdS_2$ (877.00): calcd. C 57.52, H 5.70, N 6.38; found C 57.40, H 5.55, N 6.22. **5b(SbF$_6$)$_2$**: Yield" 267.8 mg (89%). $C_{28}H_{36}F_{12}N_4PdSb_2$ (1006.24): calcd. C 33.42, H 3.58, N 5.57; found C 33.15, H 3.49, N 5.33.

NMR Spectroscopic Data for 5b(BAr′$_4$)$_2$: ^{1}H NMR (400.13 MHz, CD_2Cl_2, 21 °C): δ = 1.18 (t, $^3J_{H,H}$ = 7.6 Hz, 12 H, CH_3CH$_2$), 2.70 (q, $^3J_{H,H}$ = 7.6 Hz, 8 H, CH$_3$CH_2), 7.33 [d, $^3J_{H,H}$ = 8.8 Hz, 8 H, *m*-Ar–H(4-EtPy)], 7.59 [s, 8 H, *p*-Ar–H(BAr′$_4$)], 7.75 [s, 16 H, *o*-Ar–H(BAr′$_4$)], 8.08 [d, $^3J_{H,H}$ = 8.8 Hz, 8 H, *o*-Ar–H(4-EtPy)] ppm. ^{13}C{^{1}H} NMR (100.62 MHz, CD_2Cl_2, 21 °C): δ = 12.81 (s, *C*H$_3$CH$_2$), 28.24 (s, CH$_3$*C*H$_2$), 117.47 [s, *p*-Ar–C(BAr′$_4$)], 124.54 (q, $^1J_{C,F}$ = 272.5 Hz, *C*F$_3$C), 128.19 [s, *m*-Ar–C(4-EtPy)], 129.29 [q, $^2J_{C,F}$ = 38.7 Hz, *m*-Ar–C(BAr′$_4$)], 134.77 [s, *o*-Ar–C(BAr′$_4$)], 149.46 [s, *o*-Ar–C(4-EtPy)], 161.70 [s, *p*-Ar–C(4-EtPy)], 161.71 [m, *ipso*-Ar–C(BAr′$_4$)] ppm. This complex behaves as an 1:2 electrolyte in nitroethane (Λ_M = 115 Ω^{-1} cm^{2}mol^{-1}).[16]

NMR Spectroscopic Data for 5b(OTs)$_2$: ^{1}H NMR (400.13 MHz, CD_2Cl_2, 21 °C): δ = 1.16 (t, $^3J_{H,H}$ = 7.6 Hz, 12 H,CH_3CH$_2$), 2.41 (s, 6 H, CH$_3$), 2.61 (q, $^3J_{H,H}$ = 7.6 Hz, 8 H, CH$_3$CH_2), 7.19 [d, $^3J_{H,H}$ = 8.8 Hz, 8 H, *m*-Ar–H(4-EtPy)], 7.29 [d, $^3J_{H,H}$ = 7.6 Hz, 4 H, Ar–H(OTs)], 7.99 [s, $^3J_{H,H}$ = 7.6 Hz, 4 H, Ar–H(OTs)], 9.52 [d, $^3J_{H,H}$ = 8.8 Hz, 8 H, *o*-Ar–H(4-EtPy)] ppm. ^{13}C{^{1}H} NMR (100.62 MHz, CD_2Cl_2, 21 °C): δ = 13.26 (s, *C*H$_3$CH$_2$), 21.03 (s, CH$_3$), 27.95 (s, CH$_3$*C*H$_2$), 125.85 [s, *m*-Ar–C(4-EtPy)], 126.02 [s, Ar–C(OTs)], 128.75 [s, Ar–C(OTs)], 139.36 [s, Ar–C(OTs)], 144.85 [s, Ar–C(OTs)], 151.52 [s, *o*-Ar–C(4-EtPy)], 157.19 [s, *p*-Ar–C(4-EtPy)] ppm. This complex behaves as an 1:1 electrolyte in nitroethane (Λ_M = 58 Ω^{-1} cm^{2}mol^{-1}).[16]

NMR Spectroscopic Data for 5b(SbF$_6$)$_2$: ^{1}H NMR (400.13 MHz, CD_2Cl_2, 21 °C): δ = 1.23 (t, $^3J_{H,H}$ = 7.6 Hz, 12 H, CH_3CH$_2$), 2.71 (q, $^3J_{H,H}$ = 7.6 Hz, 8 H, CH$_3$CH_2), 7.35 (d, $^3J_{H,H}$ = 6.4 Hz, 8 H, *m*-Ar–H), 8.73 (d, $^3J_{H,H}$ = 6.4 Hz, 8 H, *o*-Ar–H) ppm. ^{13}C{^{1}H} NMR (100.62 MHz, CD_2Cl_2, 21 °C): δ = 13.17 (s, *C*H$_3$CH$_2$), 28.11 (s, CH$_3$*C*H$_2$), 126.84 (s, *m*-Ar–C), 150.35 (s, *o*-Ar–C), 159.07 (s, *p*-Ar–C) ppm.

Operando HPNMR Experiment: A solution of **5b(OTs)$_2$** (17.0 mg, 0.019 mmol) in a [D$_8$]toluene/[D$_6$]DMSO (19:1 v/v; 2.0 mL) was transferred into a 10 mm sapphire tube that was placed into a NMR spectroscopy probe at room temperature followed by the acquisition of a ^{1}H NMR spectrum at the same temperature. The sapphire tube was then removed from the NMR spectroscopy probe and K_2CO_3 (5.4 mg, 0.038 mmol) was added, followed by the acquisition of an ^{1}H NMR spectrum at room temperature. The sapphire tube was then charged with 1,2-propanediol (156.5 μL, 1.90 mmol) and again a ^{1}H NMR spectrum was acquired at the latter temperature. The sapphire was then removed again from the NMR spectroscopy probe and charged with air (300 psi), replaced in the NMR spectroscopy probe, followed by the acquisition of an ^{1}H NMR spectrum at room temperature. The NMR spectroscopy probe was then heated to 80 °C and maintained at this temperature for 1 h. During this period of time, ^{1}H NMR spectra were acquired in a time interval of 15 min. Afterwards the NMR spectroscopy probe was cooled to room temperature and a final ^{1}H NMR spectrum was acquired before removing the sapphire tube from the probe and venting off the air pressure. The NMR spectroscopic solution was then analyzed by GC–MS.

Catalytic Oxidation Reactions: Typically, the amount of precursor (0.01 mmol) and of K_2CO_3 (0.02 mmol), if used, was put at room temperature in a stainless steel autoclave (65 mL) equipped with a homemade temperature and pressure controller and a magnetic stirrer. Then a 19:1 (v/v) solvent mixture of toluene and DMSO (20 mL), substrate (1.00 mmol) and decane (100 μL) (i.e., standard) were added and the autoclave was sealed. The autoclave was then heated to 80 °C by means of an oil bath. Once the desired temperature had been reached, the autoclave was pressurized with air (300 psi) and stirring was started (600 rpm). After the desired reaction time the autoclave was successively removed from oil bath, cooled to 10 °C by means of a water/ice bath, followed by the release of the air pressure from the autoclave. Afterwards, the catalytic solution was subjected to GC and GC–MS analyses. Isolated products where obtained chromatographically.

Crystal-Structure Determination of 5b(BAr′$_4$)$_2$ and 5b(OTs)$_2$·2H$_2$O: Single crystals of **5b(BAr′$_4$)$_2$ and 5b(OTs)$_2$**·2H$_2$O suitable for a single-crystal X-ray structure analysis were obtained by diffusion of a toluene-layered solution of the corresponding compounds in dichloromethane at room temperature. Typically, a suitable crystal was mounted on a glass fibre with silicon grease and placed into the cold nitrogen stream. Diffraction data were collected with an Oxford Diffraction CCD diffractometer, using Mo-K_α radiation (λ = 0.71069 Å) and corrected for Lorentz and polarization effects. Absorption corrections were performed using the XABS2 program.[17a] All structures were solved by direct methods using SHELXS-97[17b] and refined by full-matrix least-squares methods against F^2 using the WINGX[17c] software package. All non-hydrogen atoms were refined anisotropically, whereas hydrogen atoms were added at calculated positions and refined applying a riding model with isotropic U values depending on the $U_{eq.}$ of the adja-

Table 3. Crystallographic data and structure refinement details for **5b(BAr′$_4$)$_2$** and **5b(OTs)$_2$**·2H$_2$O.

	5b(BAr′$_4$)$_2$	**5b(OTs)$_2$**·2H$_2$O
Formula	$C_{92}H_{60}B_2F_{48}N_4Pd$	$C_{42}H_{54}N_4O_8PdS_2$
M_r [g mol^{-1}]	2261.46	913.43
Crystal habit	white prism	white prism
Crystal size [mm]	0.20 × 0.20 × 0.10	0.30 × 0.20 × 0.10
T [K]	150(2)	170(2)
Crystal system	monoclinic	monoclinic
Space group	$P2_1/n$	$P2_1/c$
a [Å]	14.0605(4)	10.6103(5)
b [Å]	15.4722(4)	11.4837(4)
c [Å]	23.1075(5)	18.3511(9)
α [°]		
β [°]	100.021(3)	106.619(5)
γ [°]		
V [Å^3]	4950.3(2)	2142.6(2)
Z	2	2
$D_{calcd.}$ [g cm^{-3}]	1.517	1.416
F(000)	2256	952
Θ range [°]	4.21–29.68	4.23–30.52
Absorption coefficient [mm^{-1}]	0.324	0.586
Range of transmission factors	0.330–0.892	0.457–0.889
Reflections collected	36662	5332
Independent reflections	12272	5332
Parameters	666	270
R_1, wR_2 [$I > 2\sigma(I)$]	0.0603, 0.1586	0.0321, 0.0733
R_1, wR_2 (all data)	0.1061, 0.1779	0.0479, 0.0773
$\Delta\rho$ [e Å^{-3}]	0.981/–0.540	0.355/–0.505

cent carbon atom. Relevant crystallographic data for **5b(BAr′$_4$)$_2$** and **5b(OTs)$_2$**·2H$_2$O are compiled in Table 3.

CCDC-790283 [for **5b(BAr′$_4$)$_2$**] and -790284 [for **5b(OTs)$_2$**·2H$_2$O] contain the supplementary crystallographic data for this paper. These data can be obtained free of charge from the Cambridge Crystallographic Data Centre via www.ccdc.cam.ac.uk/data_request/cif.

Supporting Information (see footnote on the first page of this article): CP-MAS ^{13}C spectra of **1a** and **2a**; crystal-structure determination, ORTEP plots and crystallographic data for **2a**, **3b** and **4b/c**; CV study of **3a/b, 4b/c** and **5a/b(BAr′$_4$)$_2$**.

Acknowledgments

Thanks are also given to the European Commission for financing the project IDECAT (NoE contract number NMP3-CT-2005-011730).

[1] T. F. Blackburn, J. Schwartz, *J. Chem. Soc., Chem. Commun.* **1977**, 157–158.
[2] a) J. E. Bäckvall, *Modern Oxidation Methods*, Wiley-VCH, **2004**; b) J. B. Arterburn, *Tetrahedron* **2001**, *57*, 9765–9788; c) J. Muzart, *Tetrahedron* **2003**, *59*, 5789–5816.
[3] a) K. Omura, D. Swern, *Tetrahedron* **1978**, *34*, 1651–1660; b) D. B. Dess, J. C. Martin, *J. Am. Chem. Soc.* **1991**, *113*, 7277–7287.
[4] a) T. Maki, S. Iikawa, G. Mogami, H. Harasawa, Y. Matsumura, O. Onomura, *Chem. Eur. J.* **2009**, *15*, 5364–5370; b) T. Maki, K. Fukae, H. Harasawa, T. Ohishi, Y. Matsumura, O. Onomura, *Tetrahedron Lett.* **1998**, *39*, 651–654.
[5] a) S. S. Stahl, *Angew. Chem. Int. Ed.* **2004**, *43*, 3400–3420; b) N. R. Conley, L. A. Labios, D. M. Pearson, C. L. McCrory, R. W. Waymouth, *Organometallics* **2007**, *26*, 5447–5453; c) M. J. Schultz, C. C. Park, M. S. Sigman, *Chem. Commun.* **2002**, 3034–3035; d) L. Bettucci, C. Bianchini, W. Oberhauser, T.-H. Hsiao, H. M. Lee, *J. Mol. Catal. A* **2010**, *322*, 63–72; e) B. A. Steinhoff, S. S. Stahl, *Org. Lett.* **2002**, *4*, 4179–4181; f) G.-J. ten Brink, I. W. C. E. Arends, R. A. Sheldon, *Science* **2000**, *287*, 1636–1639; g) G.-J. ten Brink, I. W. C. E. Arends, M. Hoogenraad, G. Verspui, R. A. Sheldon, *Adv. Synth. Catal.* **2003**, *345*, 1341–1352; h) G.-J. ten Brink, I. W. C. E. Arends, R. A. Sheldon, *Adv. Synth. Catal.* **2002**, *344*, 355–369; i) T. Nishimura, T. Onoue, K. Ohe, S. Uemura, *J. Org. Chem.* **1999**, *64*, 6750–6755; j) M. J. Schultz, S. S. Hamilton, D. R. Jensen, M. S. Sigman, *J. Org. Chem.* **2005**, *70*, 3343–3352; k) B. A. Steinhoff, S. R. Fix, S. S. Stahl, *J. Am. Chem. Soc.* **2002**, *124*, 766–767; l) K. P. Peterson, R. C. Larock, *J. Org. Chem.* **1998**, *63*, 3185–3189; m) R. J. Nielsen, W. A. Goddard III, *J. Am. Chem. Soc.* **2006**, *128*, 9651–9669; n) T. Iwasawa, M. Tokunaga, Y. Obora, Y. Tsuji, *J. Am. Chem. Soc.* **2004**, *126*, 6554–6555; o) T. Nishimura, Y. Maeda, N. Kakiuchi, S. Uemura, *J. Chem. Soc. Perkin Trans. 1* **2000**, 4301–4305.
[6] B. A. Steinhoff, I. A. Guzel, S. S. Stahl, *J. Am. Chem. Soc.* **2004**, *126*, 11268–11278.
[7] a) D. C. Ebner, J. T. Bagdanoff, E. M. Ferreira, R. M. McFadden, D. D. Caspi, R. M. Trend, B. M. Stoltz, *Chem. Eur. J.* **2009**, *15*, 12978–12992; b) J. T. Bagdanoff, E. M. Ferreira, B. M. Stoltz, *Org. Lett.* **2003**, *5*, 835–837.
[8] a) Y. Tatsuno, T. Yoshida, S. Otsuka, *Inorg. Synth.* **1990**, *28*, 342–343; b) M. R. Churchill, R. Mason, *Nature* **1964**, *21*, 777.
[9] a) A. T. Normand, A. Stasch, L.-L. Ooi, K. J. Cavell, *Organometallics* **2008**, *27*, 6507–6520; b) S. Filipuzzi, P. S. Pregosin, A. Albinati, S. Rizzato, *Organometallics* **2008**, *27*, 437–444; c) H. M. Peng, G. Song, Y. Li, X. Li, *Inorg. Chem.* **2008**, *47*, 8031–8043.
[10] S. V. Kravtsova, I. P. Romm, A. I. Stash, V. K. Belsky, *Acta Crystallogr., Sect. C* **1996**, *52*, 2201–2204.
[11] a) E. Gavrielatos, G. Athanasellis, B. T. Heaton, A. Steiner, J. F. Bickley, O. Igglessi-Maropoulou, J. Markopoulos, *Inorg. Chim. Acta* **2001**, *351*, 21–26; b) A. R. Siedle, L. H. Pignolet, *Inorg. Chem.* **1982**, *21*, 135–141; c) W. Chen, C.-M. Liu, R.-G. Xiong, X.-Z. You, *Acta Crystallogr., Sect. C* **1997**, *53*, 1218–1220.
[12] N. Ito, T. Saji, S. Aoyagui, *Bull. Chem. Soc. Jpn.* **1985**, *58*, 2323–2326.
[13] a) J. Muzart, *Chem. Asian J.* **2006**, *1*, 508–515; b) M. M. Konnick, B. A. Gandhi, I. A. Guzei, S. S. Stahl, *Angew. Chem. Int. Ed.* **2006**, *45*, 2904–2907; c) J. M. Keith, R. J. Nielsen, J. Oxgaard, W. A. Goddard III, *J. Am. Chem. Soc.* **2005**, *127*, 13172–13179; d) M. C. Denney, N. A. Smythe, K. L. Cetto, R. A. Kemp, K. I. Goldberg, *J. Am. Chem. Soc.* **2006**, *128*, 2508–2509.
[14] A. Jutand, *Chem. Rev.* **2008**, *108*, 2300–2347.
[15] C. Bianchini, A. Meli, A. Traversi, Ital. Pay. FI A,000,025, **1997**.
[16] W. J. Geary, *Coord. Chem. Rev.* **1971**, *7*, 81–122.
[17] a) S. Parkin, B. Moezzi, H. Hope, *J. Appl. Crystallogr.* **1995**, *28*, 53–56; b) G. M. Sheldrick, *SHELX-97*, University of Göttingen, Germany, **1997**; c) L. J. Farrugia, *J. Appl. Crystallogr.* **1999**, *32*, 837–838.

Received: December 10, 2010
Published Online: March 2, 2011

